Progress In Electromagnetics Research Letters, Vol. 71, 91–96, 2017

Nonlinear Metamaterial Composite Structure with Tunable Tunneling Frequency

Tuanhui Feng*, Hongpei Han, Limin Wang, and Fei Yang

Abstract—A nonlinear metamaterial composite structure with tunable tunneling frequency is presented. Based on theoretical calculation results, a nonlinear metamaterial sandwich structure constructed by epsilon negative metamaterial (ENM), mu negative metamaterial (MNM) and nonlinear double negative metamaterial (NDNM) is designed, and its nonlinear properties are investigated. The measured results show that the tunneling frequency of the sandwich structure ENM-NDNM-MNM can be controlled conveniently by signal power.

1. INTRODUCTION

Metamaterials, including double negative metamaterials (DNM) and single negative metamaterials (SNM), have drawn intensive attention in the past few years, due to their unique electromagnetic properties and important applications [1–20]. For DNM, their permittivity and permeability are simultaneously negative. There are two kinds of SNM: one is the epsilon-negative metamaterial (ENM), in which the permittivity is negative, but the permeability is positive; the other is the mu-negative metamaterial (MNM), in which the permeability is negative, but the permittivity is positive. In DNM, the propagation of electromagnetic waves exhibits lots of unusual properties, and many important applications have been found, such as negative refraction and super-imaging, cloaking [1–6]. Contrasted to propagating modes in DNM, SNM are opaque and support only evanescent modes since their wavevectors are complex. However, some composite structures based on SNM can be transparent to electromagnetic waves and have many novel properties and important applications [7–14]. For instance, the waves can tunnel through a heterostructure constructured by the ENM and MNM, and the subwavelength resonator can be realized by the ENM-MNM heterostructure based on transmission line [7–9]. Nevertheless, the tunneling frequency is fixed and cannot be tuned once the fabrication of the subwavelength resonators is accomplished, which limits their practical applications greatly. So, it is meaningful to explore the metamaterial composite structure with tunable tunneling frequency to enlarge the applications of the SNM.

In the last decade, nonlinear metamaterials have aroused interests of many researchers [15–20]. In this paper, a new metamaterial composite structure with variable tunneling frequency is designed by introducing the nonlinear double negative metamaterial (NDNM) in the ENM-MNM heterostructure. For the sandwich structure ENM-NDNM-MNM, its tunneling frequency can be tuned conveniently by the signal power. The presented nonlinear metamaterial composite structure ENM-NDNM-MNM may be important for the design of nonlinear devices.

2. THEORETICAL CALCULATION

In [10], we find that the electromagnetic waves can tunnel through the sandwich structure MNM-Air-ENM. Here, the tunneling phenomenon in the sandwich structure constructed by the ENM, DNM and

Received 14 August 2017, Accepted 23 October 2017, Scheduled 1 November 2017
* Corresponding author: Tuanhui Feng (tuanhuifeng@xcu.edu.cn).
The authors are with the School of Electrical Engineering, Xuchang University, Xuchang 461000, China.

MNM shown in Figure 1 will be investigated by means of the transfer-matrix method. The analysis of tunneling condition is similar to [10]. Drude model is also used to describe the isotropic SNM, given as:

$$\varepsilon_A = \varepsilon_a - \frac{\alpha}{\omega^2}, \quad \mu_A = \mu_a \tag{1}$$

in ENM and

$$\varepsilon_B = \varepsilon_b, \quad \mu_B = \mu_b - \frac{\beta}{\omega^2} \tag{2}$$

in MNM. The angular frequency ω is in unit of GHz. These kinds of dispersion for ε_A and μ_B can be realized in some transmission line metamaterials [10–12, 14]. In the following calculation, we choose a set of parameters of $\varepsilon_a = \mu_b = 1$, $\mu_a = \varepsilon_b = 1$, and $\alpha = \beta = 900$. The thicknesses of ENM, MNM and DNM are assumed to be $d_A = 20$ mm, $d_B = 20$ mm and $d_C = 20$ mm, respectively. Let a transverse electric wave (the electric field lies in the y direction) be normally incident from a vacuum onto the ENM-DNM-MNM structure, as shown in Figure 1. The treatment for the transverse magnetic wave is similar. The calculated transmittance of the ENM-DNM-MNM sandwich structure is depicted in Figure 2 when the permittivity and permeability of the DNM are chosen to be $\varepsilon_C = \mu_C = -0.2$, $\varepsilon_C = \mu_C = -0.25$ and $\varepsilon_C = \mu_C = -0.3$, respectively. From Figure 2 it can be seen that the electromagnetic waves can tunnel completely through the ENM-DNM-MNM composite structure for our parameters, and the tunneling frequency shifts gradually to higher values with the decrease of the permittivity and permeability of the DNM. The results indicate that the tunneling frequency of the metamaterial composite structure can be tuned by the signal power when the DNM is replaced by the NDNM, since the permittivity and permeability of the NDNM can be tuned by the signal power.

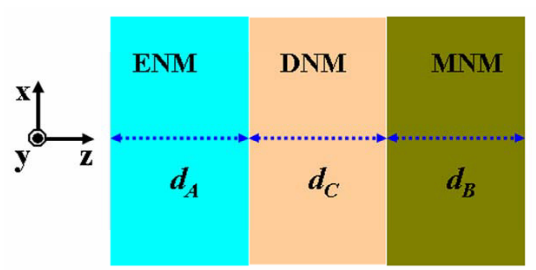

Figure 1. Schematic of the sandwich structure constructed by the ENM, DNM and MNM.

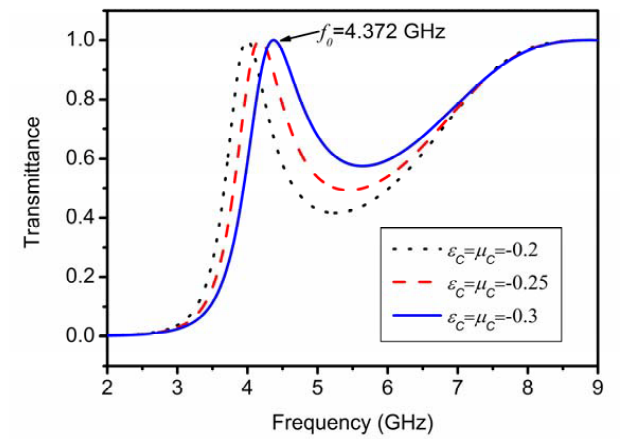

Figure 2. The calculated transmittance of the ENM-DNM-MNM sandwich structure under different values of permittivity and permeability of the DNM.

3. MICROWAVE EXPERIMENT

Based on the calculation results mentioned above, the nonlinear metamaterial composite structure constructed by the ENM, MNM and NDNM is designed by using the microstrip transmission line with lumped elements loading, as shown in Figure 3(a). In Figure 3(a), The ENM and MNM are implemented by periodically loading lumped-element series capacitors and shunt inductors on microstrip transmission line, as illustrated in [12]. Each unit cell has the same length of $d = 12$ mm, consisting of a series capacitor and a shunt inductor. For the NDNM, the series capacitors are replaced by varactor diodes, and each unit cell consists of one inductor and two varactor diodes with the same unit length of $d = 12$ mm. All varactor diodes are connected end to end or head to head. The schematics and circuit models of each unit of the ENM, MNM and NDNM are given in Figures 3(b) and 3(c). For our

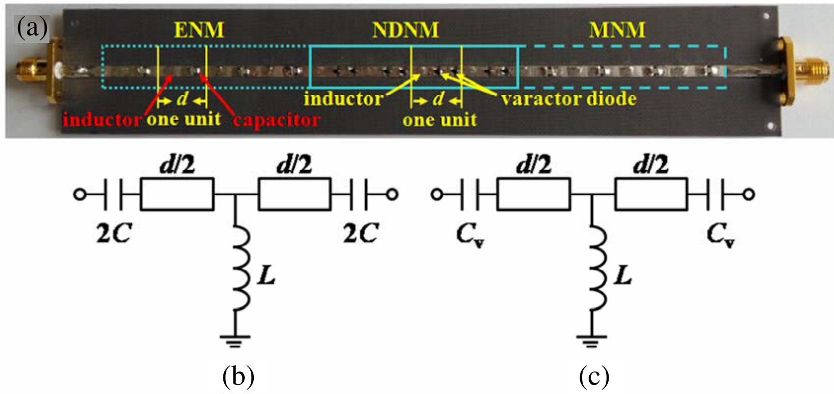

Figure 3. (a) The photograph of the nonlinear metamaterial composite structure constructed by the ENM, MNM and NDNM implemented by using the microstrip transmission line with lumped elements loading. (b) The schematic and circuit model of each unit of the ENM and MNM with the loading series capacitors (C) and shunt inductor (L). (c) The schematic and circuit model of each unit of the NDNM with the loading series varactor diodes (C_v) and shunt inductor (L).

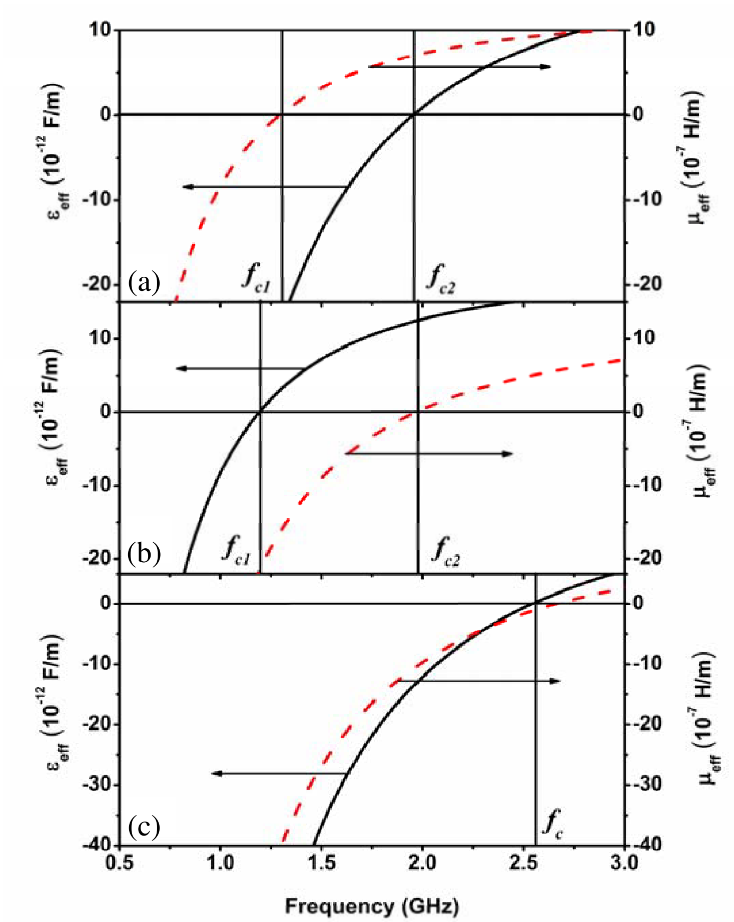

Figure 4. The calculated effective permittivity and permeability for the ENM, MNM and NDNM under the case that the voltage applied on the varactor diodes is zero.

sample, the microstrip transmission line is designed with strip width 2.73 mm to match the characteristic impedances 50 Ω. The substrate is F4B with thickness $h = 1$ mm and relative permittivity $\varepsilon_r = 2.65$. For these parameters, the distributed parameters of the microstrip transmission line are $L_0 = 248$ nH/m and $C_0 = 99$ pF/m, respectively. In the ENM, the values of the loaded series capacitors and shunt inductors are $C = 5.1$ pF and $L = 5.6$ nH, and they are $C = 2.2$ pF and $L = 15$ nH in the MNM. For the NDNM, the value of the loaded inductors is $L = 3.3$ nH. The varactor diodes of infineon BBY52 are employed, and their value is about 2.4 PF under the zero voltage.

As shown in [12], the effective permittivity and permeability can be determined by the following approximate expressions:

$$\varepsilon_{eff} \approx \left(C_0 - 1/\omega^2 Ld\right)/p, \tag{3}$$

$$\mu_{eff} \approx p\left(L_0 - 1/\omega^2 Cd\right), \tag{4}$$

where p is the structure constant of microstrip transmission line (in our experiment, its value is 5.04); L and C are the values of the loaded inductors and capacitors respectively; L_0 and C_0 are the distributed parameters of the microstrip transmission line. According to Eqs. (1) and (2), the effective permittivity and permeability of the microstrip metamaterial can be calculated. Figure 4(a) depicts the calculated results under the parameters of $C = 5.1$ pF and $L = 5.6$ nH. It can be seen that the microstrip metamaterial has $\mu_{eff} > 0$ and $\varepsilon_{eff} < 0$ in the frequency range from $f_{c1} = 1.29$ GHz to $f_{c2} = 1.96$ GHz, and obviously, the ENM is obtained in the frequency range between $f_{c1} = 1.29$ GHz and $f_{c2} = 1.96$ GHz. Similarly, Figure 4(b) illustrates the calculated results for the parameters of $C = 2.2$ pF and $L = 15$ nH. It is obvious that the microstrip metamaterial has $\mu_{eff} < 0$ and $\varepsilon_{eff} > 0$ in the frequency range between $f_{c1} = 1.19$ GHz and $f_{c2} = 1.97$ GHz, and the MNM is acquired. Figure 4(c) gives the calculation results of the NDNM under the case that the voltage applied on the varactor diodes is zero, and their capacitance value is 2.4 PF. From Figure 4(c) one can see that the microstrip metamaterial has $\mu_{eff} < 0$

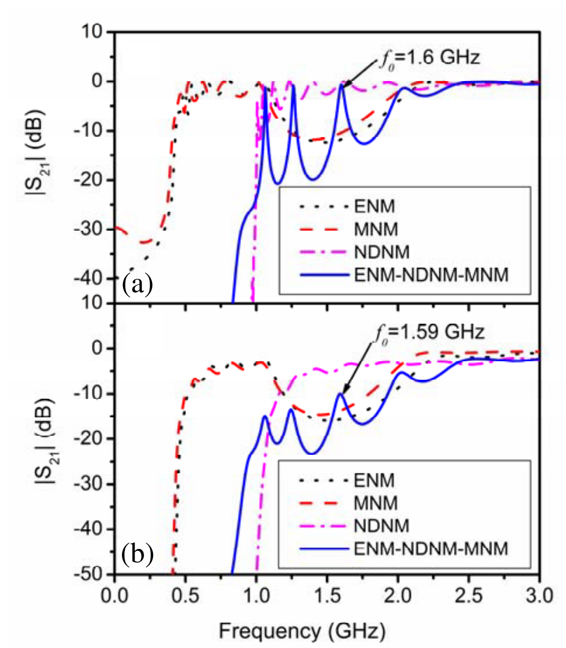

Figure 5. The simulated and measured transmission curves of the ENM, MNM, NDNM and the sandwich structure ENM-NDNM-MNM. For NDNM, the capacitance value of the varactor diodes is set to be 2.4 PF when simulated and the signal power is −5 dBm when measured.

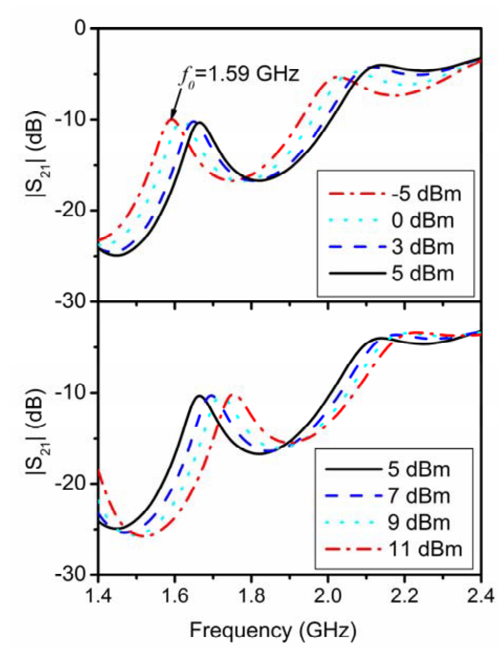

Figure 6. The measured transmission curves of the sandwich structure ENM-NDNM-MNM under different signal power.

and $\varepsilon_{eff} < 0$ in the frequency range below $f_c = 2.55\,\text{GHz}$, and the DNM is obtained. Figure 5 shows the simulated (by CST microwave studio) and measured (by Agilent vector network analyzer) transmission curves of the ENM, MNM, NDNM and the metamaterial composite structure ENM-NDNM-MNM. For NDNM, the capacitance value of the varactor diodes is set to 2.4 PF when simulated, and the signal power is $-5\,\text{dBm}$ when measured. From Figure 5, it can be seen that the stopbands of the ENM and MNM are observed, and they have accordant frequency range. The passband of the DNM also emerges, and its frequency range is greater than the ENM and MNM. Obviously, the simulated and measured results agree well with the calculation ones. For the composite structure ENM-NDNM-MNM, the tunneling phenomenon happens. The simulated result shows clearly that there exists a tunneling mode at $f_0 = 1.6\,\text{GHz}$, which agrees well with experimental observation of the tunneling mode at 1.59 GHz. It is needed to point out that the lower transmittance of the tunneling peak for experimental result is due to the energy loss of the resistance of the loaded lumped elements, for in the simulation, the resistance of the lumped elements is not considered.

Next, the tuning of tunneling frequency of the metamaterial composite structure ENM-NDNM-MNM will be investigated. Figure 6 shows the transmission curves of the sandwich structure ENM-NDNM-MNM under different signal powers. Obviously, the tunneling frequency of the sandwich structure ENM-NDNM-MNM shifts gradually to higher values with the increase of the signal power. The results indicate that the tunneling frequency of the composite structure ENM-NDNM-MNM can be controlled conveniently by signal power. Therefore, the nonlinear metamaterial composite structure ENM-NDNM-MNM may be applied in the design of nonlinear devices.

4. CONCLUSION

In conclusion, the nonlinear properties of the metamaterial composite structure ENM-NDNM-MNM are investigated. Based on the theoretical calculation results, the nonlinear sandwich structure ENM-NDNM-MNM with tunable tunneling frequency is designed, and its transmission properties with signal power are measured. The measured results show that the tunneling frequency of the sandwich structure ENM-NDNM-MNM can be controlled conveniently by power. Therefore, the nonlinear metamaterial composite structure ENM-NDNM-MNM may be important for the design of nonlinear devices.

ACKNOWLEDGMENT

This work was supported by the National Natural Science Foundation of China (Grant No. U1504110), the Aid Project for the Leading Young Teachers in Henan Provincial Institutions of Higher Education (Grant No. 2014GGJS-117), the Natural Science Foundation of Henan Province (Grant Nos. 172102210470, 15A510004, 16A140034).

REFERENCES

1. Smith, D. R. and N. Kroll, "Negative refractive index in left-handed material," *Phys. Rev. Lett.*, Vol. 85, 2933, 2000.
2. Grbic, A. and G. V. Eleftheriades, "Overcoming the diffraction limit with a planar left-handed transmission-line lens," *Phys. Rev. Lett.*, Vol. 92, 117403, 2004.
3. Pendry, J. B., D. Schurig, and D. R. Smith, "Controlling electromagnetic fields," *Science*, Vol. 312, 1780, 2006.
4. Ginis, V., P. Tassin, C. M. Soukoulis, and I. Veretennicoff, "Enhancing optical gradient forces with metamaterials," *Phys. Rev. Lett.*, Vol. 110, 057401, 2013.
5. Sreekanth, K. V., A. D. Luca, and G. Strangi, "Negative refraction in graphene-based hyperbolic metamaterials," *Appl. Phys. Lett.*, Vol. 103, 023107, 2013.
6. Henríquez, V. C., V. M. García-Chocano, and J. Sánchez-Dehesa, "Viscothermal losses in double-negative acoustic metamaterials," *Phys. Rev. Appl.*, Vol. 8, 014029, 2017.
7. Alu, A. and N. Engheta, "Pairing an epsilon-negative slab with a mu-negative slab: Resonance, tunneling and transparency," *IEEE Trans. Antennas Propagat.*, Vol. 51, 2558, 2003.

8. Fujishige, T., C. Caloz, and T. Itoh, "Experiment demonstration of transparency in the ENG-MNG pair in a CRLH transmission-line implementation," *Microwave Opt. Tech. Lett.*, Vol. 46, 476, 2005.
9. Feng, T. H., Y. H. Li, J. Y. Guo, L. He, H. Q. Li, Y. W. Zhang, Y. L. Shi, and H. Chen, "Highly localized mode in a structure made of epsilon-negative and mu-negative metamaterial," *J. Appl. Phys.*, Vol. 104, 013107, 2008.
10. Feng, T. H., Y. H. Li, H. T. Jiang, Y. Sun, L. He, H. Q. Li, Y. W. Zhang, Y. L. Shi, and H. Chen, "Electromagnetic tunneling in a sandwich structure containing single negative media," *Phys. Rev. E*, Vol. 79, 026601, 2009.
11. Jiang, H. T., H. Chen, H. Q. Li, Y. W. Zhang, J. Zi, and S. Y. Zhu, "Properties of one-dimensional photonic crystals containing single-negative materials," *Phys. Rev. E*, Vol. 69, 066607, 2004.
12. Zhang, L. W., Y. W. Zhang, L. He, H. Q. Li, and H. Chen, "Experimental study of photonic crystals consisting of ε-negative and μ-negative materials," *Phys. Rev. E*, Vol. 74, 056615, 2006.
13. Wang, Z. L., H. T. Jiang, Y. H. Li, and H. Chen, "Enhancement of self-collimated fields in photonic crystals consisting of two kinds of single-negative materials," *Opt. Express*, Vol. 18, 14311, 2010.
14. Feng, T. H., F. Yang, Y. H. Li, et al., "Light tunneling effect tuned by a meta-interface with electromagnetically-induced-transparency-like properties," *Appl. Phys. Lett.*, Vol. 102, 251908, 2013.
15. Shadrivov, I. V., A. A. Zharov, and Y. S. Kivshar, "Second-harmonic generation in nonlinear left-handed metamaterials," *J. Opt. Soc. Am. B*, Vol. 23, 529, 2006.
16. Litchinitser, N. M., I. R. Gabitov, and A. I. Maimistov, "Optical bistability in a nonlinear optical coupler with a negative index channel," *Phys. Rev. Lett.*, Vol. 99, 113902, 2007.
17. Wang, Z. Y., Y. Luo, T. Jiang, et al., "Harmonic image reconstruction assisted by a nonlinear metmaterial surface," *Phys. Rev. Lett.*, Vol. 106, 047402, 2011.
18. De Ceglia, D., M. A. Vincenti, S. Campione, et al., "Second-harmonic double-resonance cones in dispersive hyperbolic metamaterials," *Phys. Rev. B*, Vol. 89, 075123, 2014.
19. Nouri, N. and M. Zavvari, "Second-harmonic generation in iii-nitride quantum wells enhanced by metamaterials," *IEEE Photonics Technology Letters*, Vol. 28, 2199, 2016.
20. Deska, R., K. Sadecka, et al., "Nonlinear plasmonics in eutectic composites: Second harmonic generation and two-photon luminescence in a volumetric Bi_2O_3-Ag metamaterial," *Appl. Phys. Lett.*, Vol. 110, 031102, 2017.